J. Fluid Mech. (1998), *vol.* 376, *pp.* 351–375. Printed in the United Kingdom

Coriolis effect on gravity-driven convection in a rotating porous layer heated from below

By PETER VADASZ

Department of Mechanical Engineering, University of Durban-Westville, Private Bag X54001, Durban 4000, South Africa

(Received 12 February 1997 and in revised form 10 July 1998)

Linear stability and weak nonlinear theories are used to investigate analytically the Coriolis effect on three-dimensional gravity-driven convection in a rotating porous layer heated from below. Major differences as well as similarities with the corresponding problem in pure fluids (non-porous domains) are particularly highlighted. As such, it is found that, in contrast to the problem in pure fluids, overstable convection in porous media is not limited to a particular domain of Prandtl number values (in pure fluids the necessary condition is $Pr < 1$). Moreover, it is also established that in the porous-media problem the critical wavenumber in the plane containing the streamlines for stationary convection is not identical to the critical wavenumber associated with convection without rotation, and is therefore not independent of rotation, a result which is quite distinct from the corresponding pure-fluids problem. Nevertheless it is evident that in porous media, just as in the case of pure fluids subject to rotation and heated from below, the viscosity at high rotation rates has a destabilizing effect on the onset of stationary convection, i.e. the higher the viscosity the less stable the fluid. Finite-amplitude results obtained by using a weak nonlinear analysis provide differential equations for the amplitude, corresponding to both stationary and overstable convection. These amplitude equations permit one to identify from the post-transient conditions that the fluid is subject to a pitchfork bifurcation in the stationary convection case and to a Hopf bifurcation associated with the overstable convection. Heat transfer results were evaluated from the amplitude solution and are presented in terms of Nusselt number for both stationary and overstable convection. They show that rotation has in general a retarding effect on convective heat transfer, except for a narrow region of small values of the parameter containing the Prandtl number where rotation enhances the heat transfer associated with overstable convection.

1. Introduction

The study of natural convection in rotating porous media is motivated both theoretically and by its practical applications in engineering. Among the applications in engineering disciplines one can find the food process industry, chemical process industry, solidification and centrifugal casting of metals and rotating machinery. More detailed discussions of applications of natural convection in porous media and particularly in rotating porous domains are presented by Nield & Bejan (1992), Bejan (1995) in comprehensive reviews of the fundamentals of heat convection in porous media, and by Vadasz (1996*a*).

Since it is intended to compare in this paper results for convection in rotating porous media with the corresponding results in pure fluids (non-porous domains) a brief

introduction of the relevant terminology pertaining to porous media is presented in order to highlight the differences between the two. The equations governing the flow and heat transfer in porous media can be obtained via an averaging procedure of the Navier–Stokes and energy equations over a representative elementary volume (REV). As a result, the filtration velocity applicable at the macroscopic (i.e. post-averaged) level replaces the micro-level pore-scale velocity and a set of new parameters is introduced such as porosity, which appears as the ratio of the pore volume to the volume of the porous matrix, and permeability which is a property describing the ability of the porous matrix to allow fluid flow. The resulting averaged equations include a pressure gradient term and a Darcy term, the latter being proportional to the filtration velocity, $\boldsymbol{V}$, and representing the viscous forces between the fluid and the solid phases in the porous medium. An additional (Brinkman) term, proportional to $\nabla^2\boldsymbol{V}$, appears in the averaged equations representing at the macroscopic level the viscous forces between fluid particles at the pore scale, and is typically very small, i.e. $O(Da)$ (here Da is the Darcy number which is usually much smaller than unity, see definition later). There are of course additional terms, which in different circumstances can become significant, otherwise they are neglected.

Previous studies of free convection due to thermal buoyancy resulting from the *centrifugal body force* (while the gravity effect on buoyancy was neglected) deal with cases of different orientation of the temperature gradient with respect to the centrifugal force. Vadasz (1993, 1995) presented analytical solutions to the three-dimensional free-convection problem in a long rotating porous box for the case when the temperature gradient resulting from the imposed conditions on the boundaries is perpendicular to the centrifugal body force. The analysis focused on the effect of the Coriolis force on the basic free convection, resulting in secondary circulation in a plane perpendicular to the leading free-convection plane. Studies of centrifugally driven free convection with temperature gradients collinear with the centrifugal body force are limited to linear stability results. Vadasz (1994, 1996*a*) presented the stability of centrifugally driven free convection for porous layers adjacent to the axis of rotation and placed an arbitrary positive distance from the axis of rotation, respectively. Linear stability results for convection in a rotating porous layer subject to alternating direction of the centrifugal body force, a case of relevance when the axis of rotation falls within the boundaries of the porous domain, were presented by Vadasz (1996*b*).

The Coriolis effect on *gravity*-driven convection in porous media was investigated by Friedrich (1983), Jou & Liaw (1987*a*, *b*), Patil & Vaidyanathan (1983) and Palm & Tyvand (1984) for a single fluid and by Rudraiah, Shivakumara & Friedrich (1986) for a binary mixture. All these studies except Palm & Tyvand (1984) considered a porous medium model, which included the Brinkman term and/or a convective inertia term. Therefore, their governing equations were in principle similar to the Navier–Stokes equations except for an additional Darcy term proportional to the filtration velocity. Further, Rudraiah *et al.* (1986) limited their study to 'sparsely packed porous medium' and spelled out explicitly that the model validity is limited to high porosity and high permeability which makes it closer to the behaviour of a pure-fluid system (non-porous domain). It is probably for this reason that Rudraiah *et al.* (1986) preferred to use the non-porous-medium definitions for Rayleigh and Taylor numbers, which differ by a factor of Da and Da^2, respectively, from the corresponding definitions for porous media. It is because of these definitions that they concluded that for small values of Da the effect of rotation is negligible for Taylor numbers less than 10^6. If the porous-media Taylor number had been used instead, i.e. the proper porous-media scales, then one could identify significant effects of rotation at porous-media Taylor number values as

small as 10. Hence, these results are valid provided $Da = O(1)$, which is applicable for high-permeability (or sparsely packed) porous layers. Since all previously mentioned studies, except Palm & Tyvand (1984), used the same porous-medium model, this conclusion applies to them as well. On the other hand, Palm & Tyvand (1984) used an unmodified Darcy model (except for the extension to include the Coriolis term) to solve the linear stability problem of thermal convection in a porous layer subject to rotation. They discovered an important analogy showing that the onset of stationary convection in the rotating system is equivalent to the case of convection in an anisotropic porous layer. However, since they did not include the time-derivative term in the Darcy equation, they excluded the possibility of overstability (the time-derivative term is necessary when investigating wave phenomena in porous media).

In this paper an extended Darcy model is used, in the sense that the Darcy equation includes the time-derivative term which allows eventually for the convection to set in as overstability too. Brinkman as well as inertial terms are neglected, the first being significant only at a distance of $O(Da^{1/2})$ from the solid boundaries and the latter being negligible in the neighbourhood of the convection threshold, where the amplitude of the convection is expected to be small. The finite-amplitude results confirm that in the neighbourhood of the convection threshold the amplitude is proportional to the square root of the relative distance from the critical Rayleigh number. The nonlinear effects are present in this model due to the coupling between the Darcy and the energy equations, the latter including convection nonlinear terms. The objective of the present investigation is to establish the stability conditions, evaluate the three-dimensional convective solutions, including finite-amplitude results, and estimate the convective rate of heat transfer for both stationary and overstable convection in a rotating porous layer heated from below.

The corresponding results for pure fluids (non-porous domains) were presented by Chandrasekhar (1961) and Veronis (1958) for the linear stability study, and by Veronis (1958) for the finite-amplitude investigation. They showed that, in contrast to the convection problem in non-rotating systems, viscosity has a destabilizing effect on stationary convection in a rotating system at high rotation rates. The reason for this result is the tendency of small-viscosity fluids subject to rotation to horizontal two-dimensionality (i.e. Taylor–Proudman theorem), which is inconsistent with thermal convection. An additional remarkable result obtained by Veronis (1958) is the fact that the wavelength of stationary convection rolls measured in the plane containing the streamlines is independent of rotation, and equals the wavelength corresponding to convection in absence of rotation. Regarding overstable convection, it was established that a necessary condition for overstability to be at all possible is that Prandtl number must be smaller than 1. This condition limits the possible inventory of fluids for which overstability is a possible mechanism for convection to set in, e.g. water having a Prandtl number around 7 and silicon oils having much higher Prandtl numbers are all excluded.

The present study identifies the differences as well as similarities between the porous-medium and pure-fluids (non-porous domains) convection results and compares them.

2. Problem formulation and governing equations

A horizontal fluid-saturated porous layer subject to rotation is heated from below as presented in figure 1, where the vertical distance between the top and bottom boundaries is H_*. The axis of rotation and hence the coordinate system is linked to the rotating porous matrix and a negative temperature gradient in the vertical direction is

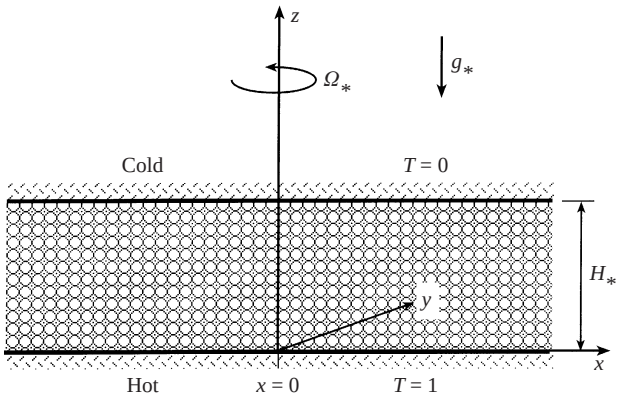

FIGURE 1. A rotating fluid saturated porous layer heated from below.

anticipated as a result of the imposed thermal boundary conditions. Not far (at distances $l_* \quad g_*/\Omega_*^2$) from the axis of rotation one can assume the gravity buoyancy to be dominant and neglect the centrifugal buoyancy, hence limiting the effect of rotation to the Coriolis acceleration and assuming the centrifugal acceleration to be constant and absorbed in the reduced pressure term. The Darcy law is extended only to include the time derivative and Coriolis terms, while the Boussinesq approximation is applied to account for the effects of the density variations. Subject to these conditions the following dimensionless set of governing equations for continuity, Darcy and energy, is obtained:

$$\boldsymbol{\nabla} \cdot \boldsymbol{V} = 0, \tag{1}$$

$$\frac{\partial \boldsymbol{V}}{\partial t'} + Ta^{1/2}\, \hat{\boldsymbol{e}}_z \times \boldsymbol{V} + \boldsymbol{V} = -\boldsymbol{\nabla} p + Ra\, T \hat{\boldsymbol{e}}_z, \tag{2}$$

$$\chi \frac{\partial T}{\partial t'} + \boldsymbol{V} \cdot \boldsymbol{\nabla} T = \nabla^2 T. \tag{3}$$

In equations (1)–(3) the values α_*/H_*, $\mu_* \alpha_*/k_*$, and $\Delta T_c = (T_H - T_C)$ are used to scale the dimensional filtration velocity components (u_*, v_*, w_*), reduced pressure (p_*), and temperature variations $(T_* - T_C)$, respectively, where α_* is the effective thermal diffusivity including the effect of the ratio between the heat capacity of the fluid and the effective heat capacity of the porous domain, μ_* is fluid's viscosity and k_* is the permeability associated with the porous matrix. The subscripts C and H stand for the cold and hot end boundaries and the subscript * denote dimensional values. The symbols $\boldsymbol{V}$, T and p represent the dimensionless filtration velocity vector, temperature and reduced pressure, respectively, and $\hat{\boldsymbol{e}}_z$ is a unit vector in the z-direction. The height of the layer H_* was used for scaling the variables x_*, y_* and z_*. Accordingly, $x = x_*/H_*$, $y = y_*/H_*$ and $z = z_*/H_*$. The time variable was scaled initially by using the value H_*^2/α_*, hence $t = t_* \alpha_*/H_*^2$, and thereafter rescaled for convenience in the form $t' = \chi t$, where χ is a dimensionless group which includes the Prandtl and Darcy numbers as well as the porosity of the porous domain and is defined as

$$\chi = \frac{\phi Pr}{Da}. \tag{4}$$

In equation (4) $Pr = \nu_*/\alpha_*$ is the Prandtl number, $Da = k_*/H_*^2$ is the Darcy number,

ϕ is porosity and ν_* stands for the kinematic viscosity of the fluid. It is only through this combined dimensionless group that the Prandtl number affects the flow in porous media. Hence, while Pr can take values from as small as 10^{-3} for liquid metals and up to 10^3 for oils, the corresponding values of χ will be magnified by a factor of ϕ/Da which is typically a big number, taking values from 10 to 10^{20}. Therefore the values of χ can be expected in the range from 10^{-2} to 10^{23}. Typical values of χ in traditional porous-media applications are quite big, a fact which provides the justification for neglecting the time-derivative term in the Darcy equation. However, in circumstances linked to modern porous-media applications its value can become of a unit order of magnitude or even smaller, in which case the time derivative term should be retained (e.g. for $Pr = 10^{-3}$, $Da = 10^{-4}$ and $\phi = 0.1$ which may be typical values within the mushy layer in solidification of binary alloys, equation (4) yields $\chi = 1$). Smaller values of ϕ corresponding to a fractured porous medium or bigger values of Da will accommodate higher Prandtl numbers or yield smaller values of χ (e.g. $Da = 10^{-2}$ 1, $\phi = 10^{-2}$, $Pr = 7$ yields $\chi = 7$). In the present case we keep the time-derivative term in the equation in order to allow for the possibility of overstable convection and will observe how the value of χ affects the frequency of overstable solutions. A linear approximation was assumed for the relationship between the density and temperature, in the form $\rho = 1-\beta T$, where $\beta = \beta_*(T_H - T_C)$ and β_* is the thermal expansion coefficient. The other dimensionless groups which appear in equation (2) are the porous-media gravity-related Rayleigh number, Ra, and the porous-media Taylor number, Ta, defined in the form

$$Ra = \frac{\beta_* \Delta T_c g_* H_* k_*}{\nu_* \alpha_*}, \quad Ta = \left(\frac{2\Omega_* k_*}{\phi \nu_*}\right)^2, \tag{5}$$

where g_* is the gravity acceleration and Ω_* is the angular velocity of rotation.

As the top and bottom boundaries are rigid, the solution must follow the impermeability conditions there, i.e. $\boldsymbol{V}\cdot\hat{\boldsymbol{e}}_n = 0$ on these boundaries, where $\hat{\boldsymbol{e}}_n$ is a unit vector normal to the boundary. The temperature boundary conditions are: $T = 1$ at $z = 0$ and $T = 0$ at $z = 1$. The lateral boundaries can be taken at the convection cell wavelength where $\boldsymbol{V}\cdot\hat{\boldsymbol{e}}_n = 0$ and $\boldsymbol{\nabla} T\cdot\hat{\boldsymbol{e}}_n = 0$.

The partial differential equations (1), (2) and (3) form a three-dimensional nonlinear coupled system which together with the corresponding boundary conditions accepts a basic motionless solution. To provide a non-trivial solution to the system it is convenient to apply the curl operator $(\boldsymbol{\nabla}\times)$ on equation (2) and obtain an equation which includes the vorticity, defined as $\boldsymbol{\omega} = \boldsymbol{\nabla}\times\boldsymbol{V}$, in the form

$$\frac{\partial \boldsymbol{\omega}}{\partial t'} + \boldsymbol{\omega} - Ta^{1/2}\frac{\partial \boldsymbol{V}}{\partial z} = Ra\left[\frac{\partial T}{\partial y}\hat{\boldsymbol{e}}_x - \frac{\partial T}{\partial x}\hat{\boldsymbol{e}}_y\right]. \tag{6}$$

It is particularly noteworthy that the vertical component of equation (6) is independent of temperature. Then, applying the curl operator again on equation (6) and using the property of $\boldsymbol{V}$ being solenoidal, which comes from equation (1), yields

$$\left[\frac{\partial}{\partial t'} + 1\right]\nabla^2 \boldsymbol{V} + Ta^{1/2}\frac{\partial \boldsymbol{\omega}}{\partial z} + Ra\left[\frac{\partial^2 T}{\partial x\,\partial z}\hat{\boldsymbol{e}}_x + \frac{\partial^2 T}{\partial y\,\partial z}\hat{\boldsymbol{e}}_y - \nabla_H^2 T\hat{\boldsymbol{e}}_z\right] = 0, \tag{7}$$

where the horizontal Laplacian operator is defined in the form $\nabla_H^2 \equiv \partial^2/\partial x^2 + \partial^2/\partial y^2$.

3. Linear stability analysis

The basic motionless solution is $\boldsymbol{V}^{(o)} = \boldsymbol{\omega}^{(o)} = 0$ and $T^{(o)} = 1 - z$. Assuming small perturbations around the basic solution in the form $\boldsymbol{V} = \boldsymbol{V}^{(o)} + \boldsymbol{V}'$, $T = T^{(o)} + T'$, and $\boldsymbol{\omega} = \boldsymbol{\omega}^{(o)} + \boldsymbol{\omega}'$ and linearizing equations (7), (3) and (6) yields the following linear system:

$$\left[\frac{\partial}{\partial t'} + 1\right]\nabla^2 \boldsymbol{V}' + Ta^{1/2}\frac{\partial \boldsymbol{\omega}'}{\partial z} + Ra\left[\frac{\partial^2 T'}{\partial x\,\partial z}\hat{\boldsymbol{e}}_x + \frac{\partial^2 T'}{\partial y\,\partial z}\hat{\boldsymbol{e}}_y - \nabla_H^2 T'\hat{\boldsymbol{e}}_z\right] = 0, \tag{8}$$

$$\left[\chi\frac{\partial}{\partial t'} - \nabla^2\right]T' - w' = 0, \tag{9}$$

$$\left[\frac{\partial}{\partial t'} + 1\right]\omega_z' = Ta^{1/2}\frac{\partial w'}{\partial z}, \tag{10}$$

where ω_z' and w' are perturbations of the vertical component of vorticity and filtration velocity respectively. The boundary conditions in the z-direction required for solving equations (8), (9) and (10) are $w' = T' = 0$ at $z = 0$ and $z = 1$. Since the layer's horizontal extent is infinite it would appear that there are no conditions necessary in this direction. However, in contrast to the problem without rotation, the presence of the axis of rotation means that it is sensible to impose symmetry conditions. It is plausible that the conditions appropriate for small centrifugal effects are the same as those for large centrifugal effects. A full investigation of this matter may be a suitable topic for further study. The coupling between equations (8), (9) and (10) can be removed by eliminating $\boldsymbol{V}'$ and $\boldsymbol{\omega}'$ to provide one equation for the temperature perturbation (or alternatively for the perturbation of vertical filtration velocity) in the form

$$\left\{\left[\frac{\partial}{\partial t'} + 1\right]^2\left[\chi\frac{\partial}{\partial t'} - \nabla^2\right]\nabla^2 + Ta\left[\chi\frac{\partial}{\partial t'} - \nabla^2\right]\frac{\partial^2}{\partial z^2} - Ra\left[\frac{\partial}{\partial t'} + 1\right]\nabla_H^2\right\}T' = 0. \tag{11}$$

Assuming an expansion into normal modes in the x- and y-directions, i.e.

$$T' = \theta(z)\exp\left[\mathrm{i}(\kappa_x x + \kappa_y y) + \sigma t'\right] + \text{c.c.}, \tag{12}$$

where c.c. stands for the complex conjugate terms, and substituting it into equation (11) provides an ordinary differential equation for $\theta(z)$ as follows:

$$\{(\sigma+1)^2[\mathrm{D}^2 - \kappa^2 - \chi\sigma](\mathrm{D}^2 - \kappa^2) + Ta[\mathrm{D}^2 - \kappa^2 - \chi\sigma]\mathrm{D}^2 - Ra(\sigma+1)\kappa^2\}\theta = 0, \tag{13}$$

where $\kappa^2 = \kappa_x^2 + \kappa_y^2$ and D^2 stands for the operator $\mathrm{d}^2/\mathrm{d}z^2$. Equation (13) yields a solution of the form $\theta = b_n \sin(n\pi z)$ which minimizes the Rayleigh number when $n = 1$, indicating that $\theta = b_1 \sin(\pi z)$ is the eigenfunction for marginal stability. Substituting this result into (13) and rescaling the parameters in the form

$$\alpha = \frac{\kappa^2}{\pi^2}, \quad R = \frac{Ra}{\pi^2}, \quad \gamma = \frac{\chi}{\pi^2} \tag{14}$$

yields the following equation for the scaled Rayleigh number, R:

$$R = \frac{[1 + \alpha + \gamma\sigma][(\sigma+1)^2(1+\alpha) + Ta]}{(\sigma+1)\alpha}. \tag{15}$$

3.1. *Stationary convection*

For stationary convection σ in equation (12) is real and for marginal stability $\sigma = 0$, therefore the corresponding characteristic values of the Rayleigh number associated with stationary convection are obtained by substituting $\sigma = 0$ in equation (15) and are presented in the form

$$R_c^{(st)} = \frac{(1+\alpha)^2}{\alpha} + Ta\frac{(1+\alpha)}{\alpha}, \tag{16}$$

where the superscript (st) denotes stationary convection. The first term in equation (16) represents the characteristic Rayleigh number for convection in the absence of rotation while the second term introduces the contribution of rotation. Minimizing $R_c^{(st)}$ with respect to α yields the critical wavenumber and the critical Rayleigh number for stationary convection

$$\alpha_{cr}^{(st)} = (Ta+1)^{1/2}, \quad R_{cr}^{(st)} = [1+(Ta+1)^{1/2}]^2. \tag{17}$$

This result is identical to the critical values presented by Palm & Tyvand (1984) and by Friedrich (1983). To observe the effect of viscosity on stability we consider the limiting conditions corresponding to $Ta \to \infty$ associated with $\Omega_* \to \infty$ or $\nu_* \to 0$. In particular we are interested in evaluating explicitly how the critical temperature difference is affected by viscosity at these limiting conditions. By using the stability condition (17) we can establish the limit as $Ta \to \infty$ in the form

$$Ta \to \infty: \quad \begin{cases} R_{cr}^{(st)} \to Ta + O(Ta^{1/2}) \\ \alpha_{cr}^{(st)} \to Ta^{1/2}. \end{cases} \tag{18}$$

Then, using the definition of the Rayleigh number and of $\beta = \beta_*(T_H - T_C)$, we can express the critical temperature difference over the porous layer as follows:

$$\beta_{cr} \to \frac{4\pi^2 k_* \alpha_* \Omega_*^2}{\phi^2 h_* g_*}\frac{1}{\nu_*} \quad \text{as } Ta \to \infty. \tag{19}$$

Equation (19) shows that the critical temperature difference for fast rotating porous domains depends on the inverse power of viscosity. This result is in contrast to the formula for the critical temperature difference obtained in the absence of rotation (when $Ta \to 0$) but it is in perfect agreement with the results of the corresponding problem in pure fluids (Chandrasekhar 1961). It implies that at high rotation rates (Ta 1) increasing the fluids' viscosity has a destabilizing effect.

With these stability results evaluated, one can proceed to present the complete eigenfunction solutions. For three-dimensional flow patterns corresponding to convection rolls whose axes are parallel to the y-direction, the variation of the variables in the y-direction vanishes, which allows the existence of a stream function, ψ, to satisfy identically the continuity equation (1). While for an infinite layer the choice of the y-direction is arbitrary, for a layer having a finite horizontal extent this direction is along the shorter horizontal dimension. Note that despite the existence of a stream function the flow is still three-dimensional and in general the component of filtration velocity in the y-direction does not vanish. Consequently $\kappa_y = 0$ and $\kappa^2 = \kappa_x^2$, which upon substitution in the solution for T' and accounting for the symmetry conditions at the axis of rotation yields for stationary convection

$$T' = B\cos(\kappa x)\sin(\pi z). \tag{20}$$

Substituting (20) into equation (9) provides the solution for w' and equations (10) and (8) provide the solution for the vertical component of vorticity ω_z', and for the horizontal components of the filtration velocity u' and v', the latter two being

$$u' = -\frac{\pi(\kappa^2+\pi^2)}{\kappa} B \sin(\kappa x)\cos(\pi z), \tag{21}$$

$$v' = \frac{\pi Ta^{1/2}(\kappa^2+\pi^2)}{\kappa} B \sin(\kappa x)\cos(\pi z). \tag{22}$$

This solution describes convection cells which are tilted in the y-direction, forming an angle $\tan^{-1}(v'/u')$ with respect to the x-axis. On this tilted plane there is no velocity component normal to the plane, and therefore this is regarded as the oblique plane containing the streamlines (see Veronis 1958 and Chandrasekhar 1961 for a graphical description of the convection pattern in the oblique plane). From equations (21) and (22) one can evaluate the ratio between the horizontal components of the filtration velocity, in the form

$$\frac{v'}{u'} = -Ta^{1/2}. \tag{23}$$

This equation, upon substitution of the critical value of the wavenumber, allows the wavenumber in the oblique plane containing streamlines to be described in the form

$$\kappa_{s,cr}^{(st)} = \kappa_{cr}^{(st)} \cos[\tan^{-1}(v'/u')] = \frac{\pi}{(1+Ta)^{1/4}}. \tag{24}$$

Equation (24) shows that the wavelength of the roll measured in the plane containing the streamlines is not independent of rotation (i.e. it is a function of Taylor number), in contrast to the corresponding problem in pure fluids (non-porous domains), where the wavelength in the oblique plane containing the streamlines was found to be identical to the value obtained for convection in absence of rotation (Veronis 1958).

3.2. *Overstable convection*

For overstable convection we allow for the possibility of oscillatory motion and therefore σ is represented in the form $\sigma = \sigma_r + i\sigma_i$. At the marginal stability state $\sigma_r = 0$ leaving only the imaginary part in the equation. Substituting $\sigma = i\sigma_i$ into equations (12) and (13) and imposing the condition $\sigma_i^2 > 0$, which is the requirement for σ_i to be real in order to get overstability possible at all, yields two algebraic equations by requiring the imaginary and the real part of equation (13) to vanish separately. This provides the solution for the characteristic values of the Rayleigh number and the frequency σ_i of the oscillations at marginal stability in the form

$$R_c^{(ov)} = \frac{2}{\alpha}\left[(1+\alpha)(1+\alpha+\gamma) + \frac{\gamma^2 Ta}{(1+\alpha+\gamma)}\right], \tag{25}$$

$$\sigma_i^2 = \frac{(1+\alpha-\gamma)\,Ta}{(1+\alpha)(1+\alpha+\gamma)} - 1, \tag{26}$$

where the superscript (ov) denotes overstable convection. At this stage it is appropriate to mention that Chandrasekhar (1961) obtained, for the corresponding convection

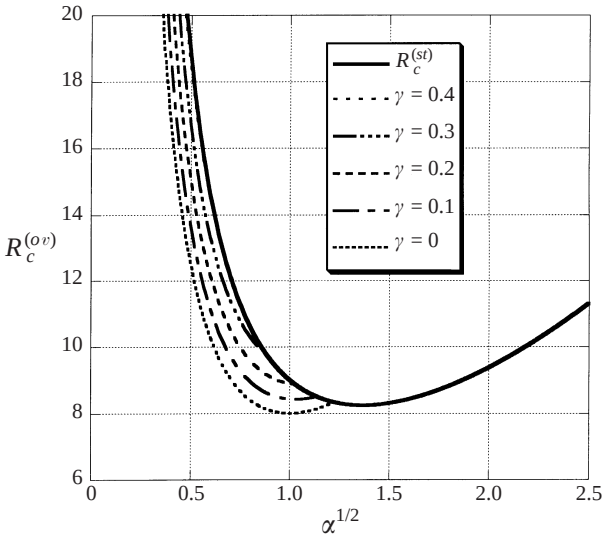

FIGURE 2. The characteristic curves representing the marginal stability limit with respect to overstable convection for $Ta = 2.5$ and different values of γ. (The continuous curve represents the upper limit corresponding to stationary convection.)

problem in pure fluids, a necessary condition for the existence of overstable solutions by imposing the condition that $\sigma_i^2 > 0$. Since in pure-fluids convection, the frequency is expressed in the form $\sigma_i^2 = [(1-Pr)/(1+Pr)][Ta/(1+\alpha)\pi^4] - (1+\alpha)^2$, it is evident that overstability cannot be established if $Pr > 1$, because this implies $\sigma_i^2 < 0$. Therefore, for pure-fluids overstability becomes possible only for values of the Prandtl number less than 1 in order to obtain real frequencies. This limits the inventory of fluids for which convection can set in as overstability in the pure-fluids problem. Equation (26) shows that in porous media the situation is completely different and no straight limitation on the Prandtl number appears as a necessary condition for overstability to set in at the convection threshold. Nevertheless, similarly to pure fluids, a further condition relating the Prandtl number (i.e. γ for the porous-media case) to the allowed range of values of Taylor number which permit overstability is derived from equation (26) by imposing the condition $\sigma_i^2 > 0$. The resulting inequality is expressed in the form $(1+\alpha)^2 + (\gamma - Ta)(1+a) + \gamma Ta < 0$, which in turn yields the following condition in order to allow a range of positive values of α that accommodate overstable convection: $0 < \gamma < (3-2\sqrt{2})\,Ta \;\forall\, Ta > 1$. Subject to this condition being fulfilled, the corresponding range of values of α which are consistent with overstable solutions is

$$\frac{(Ta-\gamma)-(Ta^2-6\gamma Ta+\gamma^2)^{1/2}}{2} < (1+\alpha) < \frac{(Ta-\gamma)+(Ta^2-6\gamma Ta+\gamma^2)^{1/2}}{2}. \quad (27)$$

Values of α lying on the boundary of the specified domain are typically consistent with values of α and the Rayleigh number on the characteristic curve associated with stationary convection. At these boundary values $\sigma_i^2 = 0$ and stationary convection takes over. The characteristic curves corresponding to $Ta = 2.5$ and plotted for different values of γ following equation (25) are presented in figure 2. The points where the overstable solutions branch off from the stationary convection curve are clearly identified. The characteristic curves associated with $Ta = 5$ and $Ta = 100$ are presented

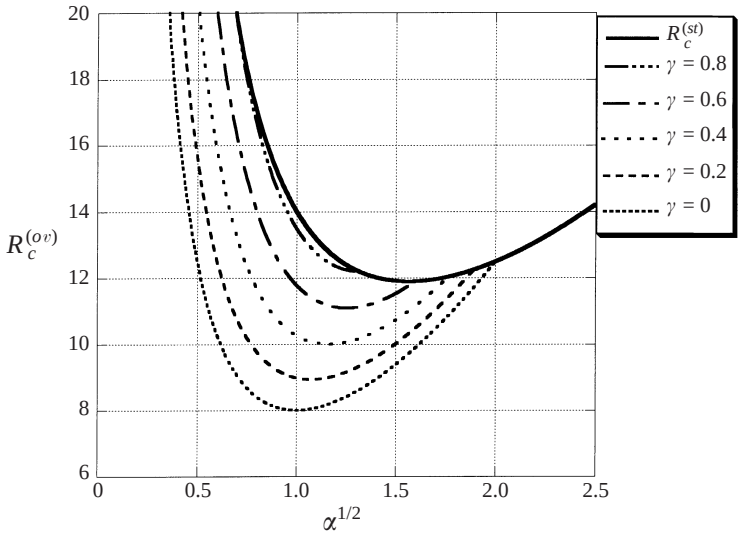

FIGURE 3. As figure 2 but for $Ta = 5$.

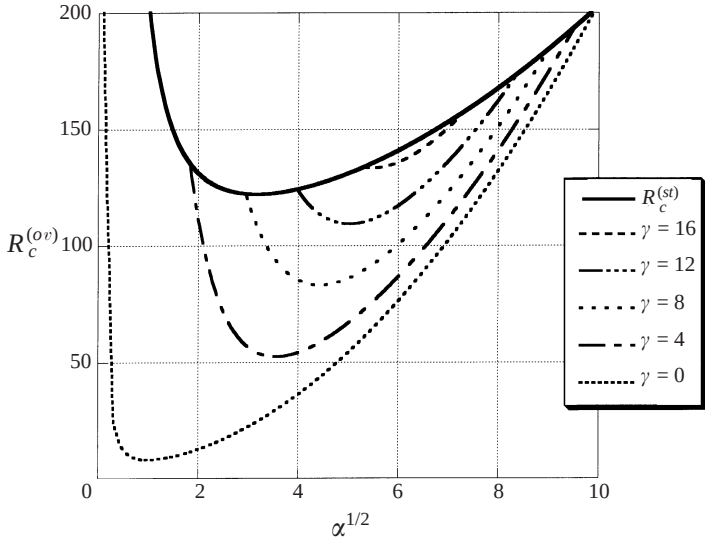

FIGURE 4. As figure 2 but for $Ta = 100$.

in figures 3 and 4, respectively, in order to observe the effect of the Taylor number on these curves.

It is worth noticing the particular case when $\gamma \to 0$, which deserves special interest because it provides a lower bound for the overstable characteristic curves. Substituting $\gamma = 0$ in equations (25) and (26) yields

$$R_c^{(ov)} = \frac{2(1+\alpha)^2}{\alpha} \quad \text{and} \quad \sigma_i^2 = \frac{Ta}{(1+\alpha)} - 1 \quad \text{for} \quad \gamma \to 0, \tag{28}$$

which indicates by minimizing $R_c^{(ov)}$ with respect to α that the critical overstable Rayleigh and wavenumbers corresponding to $\gamma = 0$ are $R_{cr}^{(ov)} = 8$ and $\alpha_{cr}^{(ov)} = 1$,

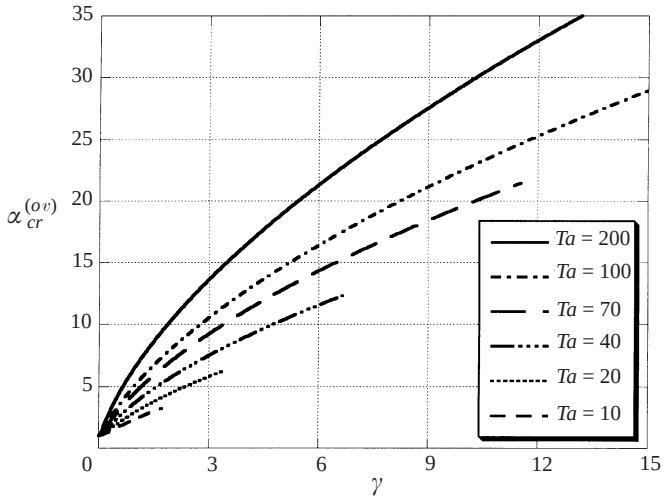

FIGURE 5. The variation of the critical values of the wavenumber, in terms of α, associated with overstable convection as a function of γ, for different values of the Taylor number.

respectively. From equation (28) it is evident that the characteristic curves for $\gamma = 0$ are independent of the Taylor number. They are therefore fixed in the $(R_c^{(ov)}, \alpha)$-plane. As such they provide the lower limit for all characteristic curves. The associated lower limit for the Taylor number is $Ta \geqslant 2$ to allow a real value for the frequency for $\alpha_{cr}^{(ov)} = 1$. However, this is not sufficient in order to have the instability setting in as overstable convection. For this to occur one must require the overstable critical Rayleigh number to be less than the corresponding stationary critical Rayleigh number, i.e. $R_{cr}^{(ov)} \leqslant R_{cr}^{(st)}$. This condition implies $Ta \geqslant 4(2-\sqrt{2})$ for $\gamma = 0$.

The other characteristic curves corresponding to different values of γ will be located in between the curve for $\gamma = 0$ and the stationary-convection characteristic curve associated with a particular value of Ta. The critical Rayleigh numbers and wavenumbers and the corresponding frequency are obtained by minimizing $R_c^{(ov)}$ in equation (25) with respect to α, a process which produces a quartic algebraic equation for $\alpha_{cr}^{(ov)}$ in the form

$$\alpha^4 + 2(\gamma+1)\alpha^3 + \gamma(\gamma+1)\alpha^2 - 2[(\gamma+1)^2 + \gamma^2 Ta]\alpha - \gamma^2(\gamma+1)Ta - (\gamma+1)^3 = 0. \quad (29)$$

The solution to equation (29) was obtained numerically, showing that only one real and positive root is associated with values of γ and Ta within the overstability limit. The others are two complex-conjugate roots and another real but negative root. The overstable critical wavenumber solution to equation (29) is presented in terms of $\alpha_{cr}^{(ov)}$ in figure 5, as a function of γ for different values of Ta. The curves end at a point where no more critical values which are consistent with $\sigma_i^2 > 0$ exist. For large values of γ this limit of end points associated with $\sigma_i^2 = 0$ can be approximated by the straight line $\alpha_{cr,max}^{(ov)} \approx 2\gamma$. By substituting the values of $\alpha_{cr}^{(ov)}$ into equation (25) one obtains the critical Rayleigh number for overstability. The variation of $R_{cr}^{(ov)}$ as a function of γ for different values of Ta is presented in figure 6, where again the curves end at the point where no more values consistent with $\sigma_i^2 > 0$ exist. For large values of γ this limit of end points $R_{cr}^{(ov)}$ associated with $\sigma_i^2 = 0$ can be approximated by the straight line $R_{cr,max}^{(ov)} \approx 8\gamma$. Substitution of the critical wavenumber solution into equation (26) yields the critical value of the frequency, which is presented in terms of $\sigma_{i,cr}^2$ in figure 7. The figure

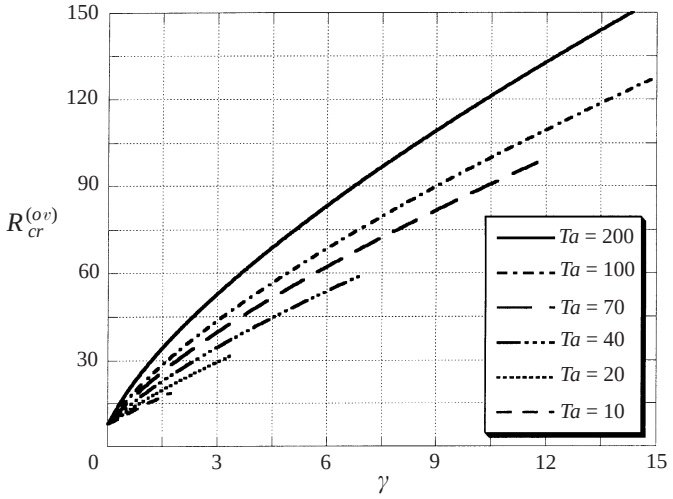

FIGURE 6. The variation of the critical values of the scaled Rayleigh number associated with overstable convection as a function of γ, for different values of the Taylor number.

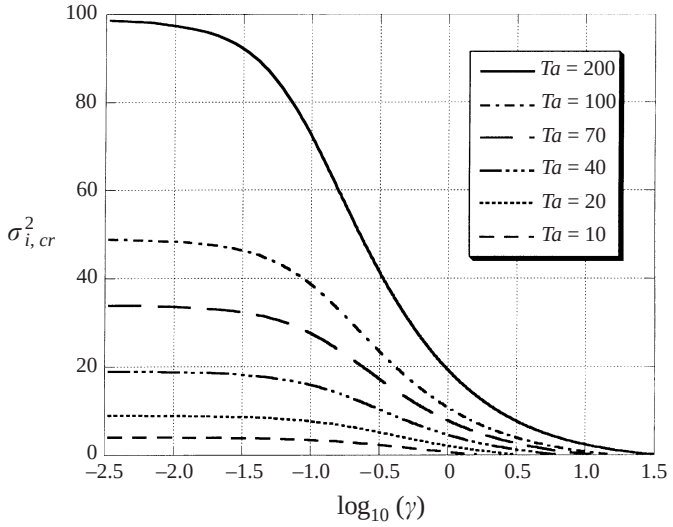

FIGURE 7. The variation of the critical values of the frequency associated with overstable convection as a function of $\log_{10}(\gamma)$, for different values of the Taylor number.

presents the frequency variation with $\log_{10}(\gamma)$ for different values of Ta. A marked increase of the frequency with increasing Taylor number is noticed from figure 7, while the large values of the frequency are particularly related to small values of γ, and they decay as γ increases. As in the case when $\gamma \to 0$, the critical curves presented in figures 5 and 6 are not sufficient for the instability to set in as overstable convection. For this to occur one must require the overstable critical Rayleigh number to be less than the corresponding stationary critical Rayleigh number, i.e. $R_{cr}^{(ov)} \leqslant R_{cr}^{(st)}$. Although the curves presented in figures 5 and 6 fulfil approximately this condition a more accurate stability map is required. This is provided in figure 8 where the (γ, Ta)-plane is divided into a zone, below the continuous curve, where the conditions are consistent with

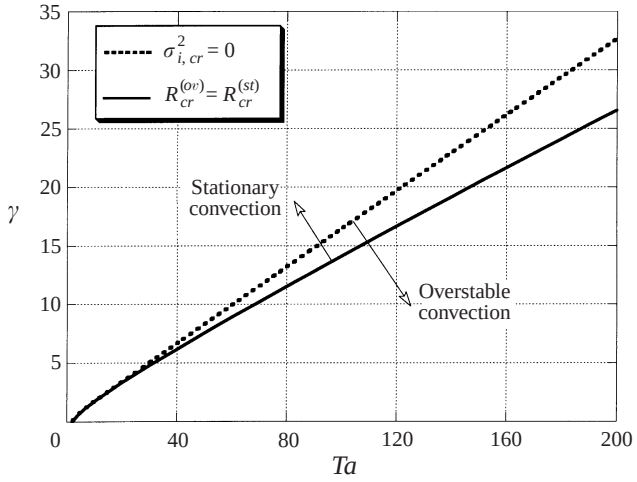

FIGURE 8. The stability map on the (γ, Ta)-plane showing the division of the plane into zones of stationary and overstable convection. The dotted line represents the limit of possible overstable convection (i.e. $\sigma_i^2 = 0$), while the continuous curve represents the limit where stationary and overstable convection occur at the same values of critical Rayleigh numbers, defining the codimension-2 point (CTP).

overstable convection, and another zone, above the continuous curve, where instability sets in as stationary convection. Below the dotted curve and above the continuous curve overstable convection is possible but will not occur because there $R_{cr}^{(ov)} > R_{cr}^{(st)}$. The dotted curve associated with $\sigma_i^2 = 0$ can be approximated for high values of γ by the straight line $Ta = 6\gamma + 2$.

4. Weak nonlinear analysis

For the weak nonlinear analysis it is convenient to use the definition of the stream function in the form $u = \partial\psi/\partial z$, $w = -\partial\psi/\partial x$, and present equations (6) and (3) in terms of the stream function and temperature, following resolution of the coupling between the components of equation (6), as follows:

$$\left[\frac{\partial}{\partial t'} + 1\right]^2 \nabla^2\psi + Ta\frac{\partial^2\psi}{\partial z^2} + Ra\left[\frac{\partial}{\partial t'} + 1\right]\frac{\partial T}{\partial x} = 0, \tag{30}$$

$$\left[\chi\frac{\partial}{\partial t'} - \nabla^2\right] T + \frac{\partial\psi}{\partial z}\frac{\partial T}{\partial x} - \frac{\partial\psi}{\partial x}\frac{\partial T}{\partial z} = 0, \tag{31}$$

where here the Laplacian definition is $\nabla^2 \equiv \partial^2/\partial x^2 + \partial^2/\partial z^2$.

The objective of the weak nonlinear analysis is to provide quantitative results regarding the amplitude of convection and consequently the heat flux for both stationary and overstable solutions. The possibility of a codimension-2 bifurcation (Brand, Hohenberg & Steinberg 1984; Cross & Kim 1988; Schöpf & Zimmermann 1993) which is anticipated at the intersection between the stationary and overstable solutions, although identified as being of significant interest for further study, is not investigated here. For investigating the solution in the neighbourhood of a codimension-2 point (CTP) a different expansion than the one we use is needed, which eventually is expected to yield an amplitude differential equation which is of second order in time.

4.1. *Expansion around stationary solutions*

The stream function and temperature are expanded in terms of a small parameter ε, defined as $\varepsilon = [Ra/Ra_{cr} - 1]^{1/2}$ following Newell & Whitehead (1969) and Segel (1969), in the form

$$[\psi, T] = [\psi^{(o)}, T^{(o)}] + \varepsilon[\psi^{(1)}, T^{(1)}] + \varepsilon^2[\psi^{(2)}, T^{(2)}] + \varepsilon^3[\psi^{(3)}, T^{(3)}] + \cdots \tag{32}$$

where $\psi^{(o)} = 0$ and $T^{(o)} = 1 - z$ represent the basic motionless solution. By using the above definition of ε, the Rayleigh number takes the form $Ra = Ra_{cr}(1 + \varepsilon^2)$ and we allow time variations only at the slow time scale $\tau = \varepsilon^2 t'$ in order to prevent exponential growth and reach finite values for the amplitude at the steady state. Slow space scales are also introduced in the form $X = \varepsilon x$, following Newell & Whitehead (1969) and Segel (1969), in order to include a continuous finite band of horizontal modes. Substituting the expansion (32) as well as the slow time and space scales in the equations (30) and (31) and equating terms which consist of like powers of ε produces a hierarchy of linear partial differential equations at each order.

At the leading order the $O(\varepsilon)$ equations are identical to the equations solved for the linear stability analysis, i.e.

$$\nabla^2\psi^{(1)} + Ta\frac{\partial^2\psi^{(1)}}{\partial z^2} + Ra_{cr}\frac{\partial T^{(1)}}{\partial x} = 0, \tag{33a}$$

$$\nabla^2 T^{(1)} - \frac{\partial\psi^{(1)}}{\partial x} = 0. \tag{33b}$$

The solution at this order is given by the eigenvalues of the stationary convection

$$\psi^{(1)} = [A_1 \mathrm{e}^{\mathrm{i}\kappa x} + A_1^* \mathrm{e}^{-\mathrm{i}\kappa x}] \sin(\pi z), \tag{34a}$$

$$T^{(1)} = [B_1 \mathrm{e}^{\mathrm{i}\kappa x} + B_1^* \mathrm{e}^{-\mathrm{i}\kappa x}] \sin(\pi z), \tag{34b}$$

where $*$ denotes complex conjugate terms and the amplitudes $A_1(\tau, X)$, $A_1^*(\tau, X)$, $B_1(\tau, X)$ and $B_1^*(\tau, X)$ are allowed to vary over the slow time and space scales. The relationship between the amplitudes is obtained by substituting the solutions (34*a*, *b*) into (33*a*, *b*), as follows:

$$B_1 = -\frac{\mathrm{i}\alpha^{1/2}}{\pi(\alpha+1)} A_1, \quad B_1^* = \frac{\mathrm{i}\alpha^{1/2}}{\pi(\alpha+1)} A_1^*. \tag{35}$$

The amplitudes A_1, A_1^* remain undetermined at this stage; they will be established from a solvability condition of the $O(\varepsilon^3)$ equations at order ε^3.

At order ε^2 the $O(\varepsilon^2)$ equations are

$$\nabla^2\psi^{(2)} + Ta\frac{\partial^2\psi^{(2)}}{\partial z^2} + Ra_{cr}\frac{\partial T^{(2)}}{\partial x} = -2\frac{\partial}{\partial X}\frac{\partial\psi^{(1)}}{\partial x} - Ra_{cr}\frac{\partial T^{(1)}}{\partial X}, \tag{36a}$$

$$\nabla^2 T^{(2)} - \frac{\partial\psi^{(2)}}{\partial x} = -2\frac{\partial}{\partial X}\frac{\partial T^{(1)}}{\partial x} - \frac{\partial\psi^{(1)}}{\partial X} + \frac{\partial\psi^{(1)}}{\partial z}\frac{\partial T^{(1)}}{\partial x} - \frac{\partial\psi^{(1)}}{\partial x}\frac{\partial T^{(1)}}{\partial z}, \tag{36b}$$

where the right-hand side of (36*a*, *b*) represents the non-homogeneous part consisting of terms which include the known solutions evaluated at the leading order, ε. These

non-homogeneous terms force a particular solution in addition to the solution of the homogeneous operator. De-coupling the equations and working out the particular solutions yields the following complete solution at this order:

$$\psi^{(2)} = [A_2 \,\mathrm{e}^{\mathrm{i}\kappa x} + A_2^* \,\mathrm{e}^{-\mathrm{i}\kappa x}] \sin(\pi z), \tag{37a}$$

$$T^{(2)} = [B_2 \,\mathrm{e}^{\mathrm{i}\kappa x} + B_2^* \,\mathrm{e}^{-\mathrm{i}\kappa x}] \sin(\pi z) - \frac{\alpha}{2\pi(\alpha+1)} A_1 A_1^* \sin(2\pi z), \tag{37b}$$

where the relationship between the amplitudes B_2 and A_2 is identical to equation (35).

The equations at order ε^3 are

$$\nabla^2\psi^{(3)} + Ta\frac{\partial^2\psi^{(3)}}{\partial z^2} + Ra_{cr}\frac{\partial T^{(3)}}{\partial x} = -2\frac{\partial}{\partial\tau}(\nabla^2\psi^{(1)}) - Ra_{cr}\frac{\partial}{\partial\tau}\left(\frac{\partial T^{(1)}}{\partial x}\right) - Ra_{cr}\frac{\partial T^{(1)}}{\partial x} - \frac{\partial^2\psi^{(1)}}{\partial X^2} - 2\frac{\partial}{\partial X}\frac{\partial\psi^{(2)}}{\partial x} - Ra_{cr}\frac{\partial T^{(2)}}{\partial X}, \tag{38a}$$

$$\nabla^2 T^{(3)} - \frac{\partial\psi^{(3)}}{\partial x} = \chi\frac{\partial T^{(1)}}{\partial\tau} + \frac{\partial\psi^{(2)}}{\partial z}\frac{\partial T^{(1)}}{\partial x} + \frac{\partial\psi^{(1)}}{\partial z}\frac{\partial T^{(2)}}{\partial x} - \frac{\partial\psi^{(2)}}{\partial x}\frac{\partial T^{(1)}}{\partial z} - \frac{\partial\psi^{(1)}}{\partial x}\frac{\partial T^{(2)}}{\partial z} - 2\frac{\partial}{\partial X}\frac{\partial T^{(2)}}{\partial x} + \frac{\partial\psi^{(2)}}{\partial X} - \frac{\partial^2 T^{(1)}}{\partial X^2} + \frac{\partial\psi^{(1)}}{\partial z}\frac{\partial T^{(1)}}{\partial X} - \frac{\partial\psi^{(1)}}{\partial X}\frac{\partial T^{(1)}}{\partial z}. \tag{38b}$$

The right-hand side of (38*a*, *b*) consists of known solutions evaluated at orders ε and ε^2 and the differential operator of the system of equations (38*a*, *b*) is identical to the operator of the equation at order ε. Since (38*a*, *b*) at order ε^3 are non-homogeneous versions of the equations at order ε, a solvability condition for the equations at ε^3 must be satisfied. This constrains the amplitude of the solution at order ε and enables its determination. The solvability condition is derived by de-coupling the equations and evaluating the right-hand-side forcing functions. The relevant forcing term has the form $[A_1 \exp(\mathrm{i}\kappa x) + A_1^* \exp(-\mathrm{i}\kappa x)] \sin(\pi z)$, the others including higher harmonics of z which do not contain the eigenfunctions corresponding to the homogeneous operator with homogeneous boundary conditions. By imposing the condition that the coefficient of the relevant forcing term must vanish one obtains the solvability condition in the form of the following partial differential equation for the complex $O(\varepsilon)$ amplitude:

$$\eta\frac{\partial A}{\partial t} - (1+\alpha)\frac{\partial^2 A}{\partial x^2} = \frac{\pi^2\alpha^2}{2}[\xi_{st}^o - AA^*]\,A, \tag{39}$$

where $A = \varepsilon A_1$, $A^* = \varepsilon A_1^*$, the original time and space scales are used, i.e. $t = t'/\chi$, and the following notation was introduced:

$$\xi_{st}^o = \frac{2(\alpha+1)}{\alpha}\left[\frac{R}{R_{cr}^{(st)}} - 1\right], \quad \eta = \frac{(\alpha+1)(2-\alpha)+\alpha\gamma}{\gamma}. \tag{40}$$

The slow space scales lead to the appearance of a diffusion term in the amplitude equation. However, the imposition of the symmetry conditions at the axis of rotation ($x = 0$) leads to the requirement $A_1 = -A_1^*$, and then the $O(\varepsilon)$ solution is reduced to the form

$$\psi^{(1)} = C_1 \sin(\kappa x) \sin(\pi z), \tag{41}$$

where $C_1 = \mathrm{i}2A_1$. This result satisfies the equations and all boundary conditions. A phase angle is not involved, and a solution without slow space scales is possible. The

diffusion term drops out of equation (39), which then transforms to the following ordinary differential equation for the real amplitude C_1:

$$\eta \frac{\mathrm{d}C}{\mathrm{d}t} = \frac{\pi^2\alpha^2}{8}[\xi_{st} - C^2]\, C, \tag{42}$$

where $C = \varepsilon C_1$ and $\xi_{st} = 4\xi^o_{st}$. Equation (42) yields the following solutions at the steady state:

$$C = \begin{cases} 0 & \forall\, R < R^{(st)}_{cr} \\ \pm \xi^{1/2}_{st} & \forall\, R \geqslant R^{(st)}_{cr}. \end{cases} \tag{43}$$

The steady amplitude solution (43) shows that a pitchfork bifurcation occurs at the critical value of the Rayleigh number associated with stationary convection. The relaxation time η is positive as long as $\gamma > \gamma^{(st)}_t$ where

$$\gamma^{(st)}_t = (1+Ta)^{1/2} - \frac{2}{(1+Ta)^{1/2}} - 1. \tag{44}$$

Below this transition value of γ the relaxation time is negative and the solution decays to the trivial value $C = 0$. The values of the Taylor number consistent with the condition of a positive relaxation time, i.e. which yields $\gamma^{(st)}_t \geqslant 0$, are represented by the condition $Ta \geqslant 3$. The determination of the amplitude provides the complete solution of the stationary convection problem at order ε. The evaluation of the heat flux by using the amplitude results from equations (39) and (43) is presented in §4.3.

4.2. *Expansion around overstable solutions*

Equations (30) and (31) are still applicable for the weak nonlinear analysis of the overstable convection. The expansion (32) is valid as well, with the only difference that here we refer to the corresponding critical values consistent with overstable convection. We introduce the slow time scales $\tau = \varepsilon^2 t'$ and $\tau_o = \varepsilon t'$, but allow the short time scale t' to be present in order to represent the amplitude fluctuations. We further rescale the short time scale in the form $\tilde{t} = \sigma_o t'$ where we used the notation $\sigma_o = \sigma^{(cr)}_i$. Substituting these expansions into (30) and (31) yields at the leading order the following equations:

$$\left[\sigma_o \frac{\partial}{\partial \tilde{t}} + 1\right]^2 \nabla^2 \psi^{(1)} + Ta \frac{\partial^2 \psi^{(1)}}{\partial z^2} + Ra_{cr}\left[\sigma_o \frac{\partial}{\partial \tilde{t}} + 1\right] \frac{\partial T^{(1)}}{\partial x} = 0, \tag{45a}$$

$$\left[\chi \sigma_o \frac{\partial}{\partial \tilde{t}} - \nabla^2\right] T^{(1)} + \frac{\partial \psi^{(1)}}{\partial x} = 0. \tag{45b}$$

The general solution for $\psi^{(1)}$ has the form

$$\psi^{(1)} = [A_1 \mathrm{e}^{\mathrm{i}(\kappa x + \tilde{t})} + B_1 \mathrm{e}^{\mathrm{i}(\kappa x - \tilde{t})} + A^*_1 \mathrm{e}^{-\mathrm{i}(\kappa x + \tilde{t})} + B^*_1 \mathrm{e}^{-\mathrm{i}(\kappa x - \tilde{t})}] \sin(\pi z), \tag{46}$$

where the amplitudes $A_1(\tau_o, \tau, X)$ and $B_1(\tau_o, \tau, X)$ describe modulations of the waves on the slow time ($\tau_o = \varepsilon t', \tau = \varepsilon^2 t'$) and space ($X = \varepsilon x$) scales for a Hopf bifurcation. This form of the solution represents travelling waves. The special cases of a pure left-travelling wave ($B_1 = 0$) or a pure right-travelling wave ($A_1 = 0$) and of standing waves ($A_1 = \pm B_1$ or $A_1 = \pm B^*_1$) can be recovered. This general solution will eventually provide two coupled equations for the complex amplitudes (Schöpf & Zimmermann 1993). However, by imposing the symmetry condition at the axis of rotation at the eigenvalues level, implying that $\psi^{(1)} = 0$ at $x = 0$, yields upon substitution in equation (46) $B^*_1 = -A_1$ and $B_1 = -A^*_1$. This result shows that the symmetry condition at the origin imposes the special case of standing waves while travelling waves are excluded.

On similar grounds as for stationary convection we can exclude the slow space scale which prevents the appearance of a diffusion term in the amplitude equation. The solution for the stream function at this order therefore takes the form

$$\psi^{(1)} = 2\mathrm{i}[A_1\,\mathrm{e}^{\mathrm{i}\tilde{t}} + A_1^*\,\mathrm{e}^{-\mathrm{i}\tilde{t}}]\sin(\kappa x)\sin(\pi z),$$
$$T^{(1)} = 2[C_1\,\mathrm{e}^{\mathrm{i}\tilde{t}} + C_1^*\,\mathrm{e}^{-\mathrm{i}\tilde{t}}]\cos(\kappa x)\sin(\pi z), \tag{47b}$$

which is similar to Steinberg & Brand (1984) for convection in a reactive mixture in a porous medium. The relationship between the coefficients is obtained as follows:

$$C_1 = -\frac{\alpha^{1/2}[\gamma\sigma_o + \mathrm{i}(\alpha+1)]}{\pi[(\alpha+1)^2+\gamma^2\sigma_o^2]}A_1, \tag{48a}$$

$$C_1^* = -\frac{\alpha^{1/2}[\gamma\sigma_o - \mathrm{i}(\alpha+1)]}{\pi[(\alpha+1)^2+\gamma^2\sigma_o^2]}A_1^*. \tag{48b}$$

The equations at order ε^2 are

$$\left[\sigma_o\frac{\partial}{\partial\tilde{t}}+1\right]^2\nabla^2\psi^{(2)} + Ta\frac{\partial^2\psi^{(2)}}{\partial z^2} + Ra_{cr}\left[\sigma_o\frac{\partial}{\partial\tilde{t}}+1\right]\frac{\partial T^{(2)}}{\partial x}$$
$$= -2\frac{\partial}{\partial\tau_o}\left[\sigma_o\frac{\partial}{\partial\tilde{t}}+1\right]\nabla^2\psi^{(1)} - Ra_{cr}\frac{\partial}{\partial\tau_o}\left(\frac{\partial T^{(1)}}{\partial x}\right), \tag{49a}$$

$$\left[\chi\sigma_o\frac{\partial}{\partial\tilde{t}} - \nabla^2\right]T^{(2)} + \frac{\partial\psi^{(2)}}{\partial x} = -\chi\frac{\partial T^{(1)}}{\partial\tau_o} - \frac{\partial\psi^{(1)}}{\partial z}\frac{\partial T^{(1)}}{\partial x} + \frac{\partial\psi^{(1)}}{\partial x}\frac{\partial T^{(1)}}{\partial z}. \tag{49b}$$

The solution to the system (49*a*, *b*) is the superposition of a homogeneous part and the particular solutions arising from the non-homogeneous terms in the right-hand side of the equations, which are known from the order-ε solutions. The homogeneous part of the solution is similar to the solutions at order ε since the homogeneous operator is the same. Therefore

$$\psi_h^{(2)} = 2\mathrm{i}[A_2\,\mathrm{e}^{\mathrm{i}\tilde{t}} + A_2^*\,\mathrm{e}^{-\mathrm{i}\tilde{t}}]\sin(\kappa x)\sin(\pi z), \tag{50a}$$
$$T_h^{(2)} = 2[C_2\,\mathrm{e}^{\mathrm{i}\tilde{t}} + C_2^*\,\mathrm{e}^{-\mathrm{i}\tilde{t}}]\cos(\kappa x)\sin(\pi z), \tag{50b}$$

while the relationship between the coefficients is identical to equation (48). When evaluating the right-hand side of (49*a*, *b*) in order to obtain the particular solutions, it becomes clear that these non-homogeneous terms will produce particular solutions of the form $\tilde{t}\sin(\tilde{t})\sin(\kappa x)\sin(\pi z)$ or $\tilde{t}\cos(\tilde{t})\sin(\kappa x)\sin(\pi z)$ which are secular terms in the solution, i.e. we have a condition of resonance, unless $\partial A_1/\partial\tau_o = 0$. To avoid resonance we obtain the particular solutions by setting $\partial A_1/\partial\tau_o = 0$. The particular solution for the stream function vanishes, i.e. $\psi_p^{(2)} = 0$, and the particular solution for the temperature is

$$T_p^{(2)} = [b_2 + a_1\,\mathrm{e}^{2\mathrm{i}\tilde{t}} + a_1^*\,\mathrm{e}^{-2\mathrm{i}\tilde{t}}]\sin(2\pi z), \tag{51}$$

where the coefficients b_2, a_1 and a_1^* are related to the amplitude at order ε as follows:

$$b_2 = -\frac{\alpha(\alpha+1)}{\pi[(\alpha+1)^2+\gamma^2\sigma_o^2]}A_1A_1^*, \tag{52a}$$

$$a_1 = \frac{\alpha[2(\alpha+1)-\gamma^2\sigma_o^2-\mathrm{i}\gamma\sigma_o(\alpha+3)]}{\pi[(\alpha+1)^2+\gamma^2\sigma_o^2](4+\gamma^2\sigma_o^2)}(A_1)^2, \tag{52b}$$

$$a_1^* = \frac{\alpha[2(\alpha+1)-\gamma^2\sigma_o^2+\mathrm{i}\gamma\sigma_o(\alpha+3)]}{\pi[(\alpha+1)^2+\gamma^2\sigma_o^2](4+\gamma^2\sigma_o^2)}(A_1^*)^2. \tag{52c}$$

The complete solution at this order is therefore $\psi^{(2)} = \psi_h^{(2)}$ and $T^{(2)} = T_h^{(2)} + T_p^{(2)}$.

The equations at order ε^3 were de-coupled to yield one equation for the stream function in the form

$$\left\{\left[\chi\sigma_o\frac{\partial}{\partial\tilde{t}}-\nabla^2\right]\left[\left(\sigma_o\frac{\partial}{\partial\tilde{t}}+1\right)^2\nabla^2+Ta\frac{\partial^2}{\partial z^2}\right]-Ra_{cr}\left[\sigma_o\frac{\partial}{\partial\tilde{t}}+1\right]\frac{\partial^2}{\partial x^2}\right\}\psi^{(3)}=\text{RHS}, \quad (53)$$

where RHS stands for the right-hand-side terms which have been evaluated from previously known solutions at orders ε and ε^2. The algebra involved in the solutions at this order is so tedious and long that only the results will be outlined here. In principle, in order to avoid resonant terms to appear in the solutions, the coefficients of the corresponding forcing terms producing resonance should be set equal to 0. The two relevant forcing terms have the form $e^{i\tilde{t}}\sin(\kappa x)\sin(\pi z)$ and $e^{-i\tilde{t}}\sin(\kappa x)\sin(\pi z)$, the others including non-resonant harmonics or convection modes different to the natural modes associated with the homogeneous operator with homogeneous boundary conditions. Setting the coefficients of the resonant terms equal to zero yields an equation for the unknown complex amplitude of the convection at order ε in the form

$$\frac{dA}{dt}=h_{21}[\xi_{ov}-h_{32}AA^*]A, \quad (54)$$

where $A=\varepsilon A_1$, $A^*=\varepsilon A_1^*$, the original time scale is used, i.e. $t=t'/\chi$, and the following notation was introduced:

$$\xi_{ov}=\varepsilon^2=\left[\frac{R}{R_{cr}^{(ov)}}-1\right], \quad h_{21}=h_{21}^o+im_{21}, \quad h_{31}=h_{31}^o+im_{31}, \quad (55)$$

while the definitions of $h_{32}, h_{21}^o, m_{21}, h_{31}^o$ and m_{31} are

$$h_{32}=\frac{\alpha[6(\alpha+1)+\gamma^2\sigma_o^2\alpha-i\gamma\sigma_o(\alpha+3)]}{(4+\gamma^2\sigma_o^2)[(\alpha+1)^2+\gamma^2\sigma_o^2]}, \quad (56a)$$

$$h_{21}^o=\frac{\pi^2\gamma\alpha R_c s^\circ}{q^\circ}[p^\circ(\sigma_o^2+1)(2s^\circ p^\circ+\alpha R_c\gamma)-\alpha R_c s^\circ], \quad (56b)$$

$$m_{21}=-\frac{\pi^2\gamma\alpha R_c s^\circ\sigma_o}{q^\circ}[2s^\circ p^\circ\gamma(\sigma_o^2+1)+\alpha R_c(p^{\circ 2}-\gamma^2)], \quad (56c)$$

$$\begin{aligned}h_{31}^o=\frac{\pi^2\gamma\alpha^2R_c}{(4+\gamma^2\sigma_o^2)q^\circ}\{&(6p^\circ+\gamma^2\sigma_o^2\alpha)[p^\circ(\sigma_o^2+1)(2s^\circ p^\circ+\alpha R_c\gamma)-\alpha R_c s^\circ]\\&-\gamma\sigma_o^2(p^\circ+2)[2s^\circ p^\circ\gamma(\sigma_o^2+1)+\alpha R_c(p^{\circ 2}-\gamma^2)]\}, \quad (56d)\end{aligned}$$

$$\begin{aligned}m_{31}=-\frac{\pi^2\gamma\alpha^2R_c\sigma_o}{(4+\gamma^2\sigma_0^2)q^\circ}\{&\gamma(p^\circ+2)[p^\circ(\sigma_o^2+1)(2s^\circ p^\circ+\alpha R_c\gamma)-\alpha R_c s^\circ]\\&+(6p^\circ+\gamma^2\sigma_o^2\alpha)[2s^\circ p^\circ\gamma(\sigma_o^2+1)+\alpha R_c(p^{\circ 2}-\gamma^2)]\}, \quad (56e)\end{aligned}$$

where p°, q° and s° are defined in the form

$$\left.\begin{aligned}&p^\circ=(1+\alpha), \quad s^\circ=(1+\alpha)^2+\gamma^2\sigma_o^2,\\&q^\circ=\sigma_o^2[2s^\circ p^\circ(p^\circ+\gamma)+\gamma\alpha R_c(p^\circ-\gamma)]^2+p^{\circ 2}[\alpha R_c(p^\circ-\gamma)-2s^\circ(p^\circ-\gamma\sigma_o^2)]^2.\end{aligned}\right\} \quad (57)$$

It is convenient to present equation (54) for the complex amplitude as a set of two equations for the absolute value of the amplitude ($r=|A|$) and its phase (θ) in the form

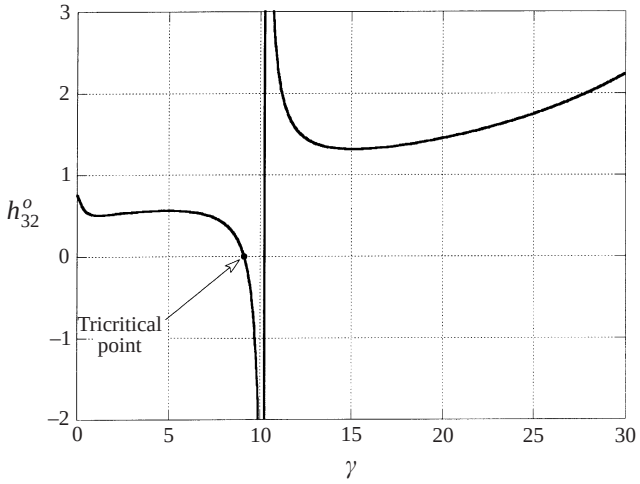

FIGURE 9. Finite-amplitude results for overstable convection: variation of the nonlinear term coefficient, h_{32}^o as a function of γ for $Ta = 60$, identifying the tricritical point γ_{tc} where h_{32}^o changes sign. For values of γ below the tricritical point the bifurcation is forward, while for $\gamma > \gamma_{tc}$ the bifurcation is inverse. The value of γ were a singularity causes h_{32}^o to diverge is beyond the overstability limit, i.e. it occurs always at $\gamma > \gamma_{max}$.

$$A = r\,\mathrm{e}^{\mathrm{i}\theta}, \quad A^* = r\,\mathrm{e}^{-\mathrm{i}\theta} \tag{58}$$

with $AA^* = r^2$ and

$$h_{12}^o \frac{\mathrm{d}r}{\mathrm{d}t} = [\xi_{ov} - h_{32}^o r^2]\, r, \tag{59}$$

$$\frac{\mathrm{d}\theta}{\mathrm{d}t} = m_{21}\,\xi_{ov} - m_{31}\, r^2, \tag{60}$$

where $h_{12}^o = 1/h_{21}^o$ and $h_{32}^o = h_{31}^o/h_{21}^o$. The sign of the coefficient of the nonlinear term, i.e. h_{32}^o indicates whether the bifurcation is forward or inverse. When $h_{32}^o > 0$ the bifurcation is forward while a negative value of h_{32}^o suggests an inverse bifurcation. The point where h_{32}^o changes sign is identified as the (non-equilibrium) tricritical point (because of the many similarities the present problem shares with thermodynamic equilibrium phase transitions). Calculating h_{32}^o over the parameter domain considered yields a graphical pattern as presented in figure 9, for $Ta = 60$. For this value of the Taylor number, the maximum allowed value of γ which is consistent with overstable convection (i.e. with $\sigma_o^2 \geqslant 0$) is $\gamma_{max} = 9.92$. Therefore, from figure 9 one observes that the bifurcation is forward (i.e. $h_{32}^o > 0$) for most of the parameter domain, i.e. for $\gamma < \gamma_{tc}$, where γ_{tc} is the value of γ at the tricritical point, and becomes inverse for $\gamma_{tc} < \gamma < \gamma_{max}$, actually in the neighbourhood of the codimension-2 point (CTP) but not exactly at the CTP. In general h_{32}^o changes sign again via a singularity, however this is always beyond the overstability limit. Actually there is at least another zero of h_{32}^o at very high values of γ which is also not relevant to the problem because it happens outside the overstability domain (i.e. at $\gamma > \gamma_{max}$). The general behaviour of h_{32}^o is the same for all values of Ta considered, except for the location of the tricritical point. For the case presented in figure 9 (corresponding to $Ta = 60$) the tricritical point γ_{tc} is below γ_{max}. This, however, is not the case for all values of Ta. The location of γ_{tc} and γ_{max} as a function Ta is presented in figure 10. From the figure it is evident that there

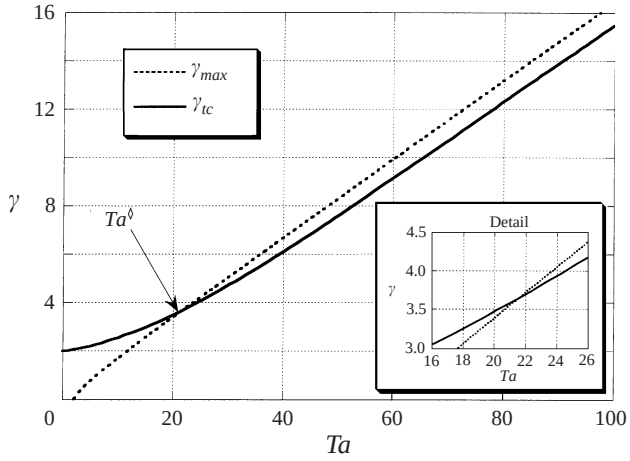

FIGURE 10. Finite-amplitude results for overstable convection: Maximum and tricritical values of γ as a function of Taylor number. The inset shows the detail of their intersection where $\gamma_{tc} = \gamma_{max} = \gamma^{\diamond}$ and $Ta = Ta^{\diamond}$. For Taylor numbers above $Ta^{\diamond}$: $\gamma_{tc} < \gamma_{max}$, while for Taylor numbers below $Ta^{\diamond}$: $\gamma_{tc} > \gamma_{max}$.

is a value of the Taylor number, say $Ta^{\diamond}$ (and its corresponding value of γ, say $\gamma^{\diamond}$) above which $\gamma_{tc} < \gamma_{max}$ and below it $\gamma_{tc} > \gamma_{max}$ (at $Ta = Ta^{\diamond}$, $\gamma_{tc} = \gamma_{max} = \gamma^{\diamond}$). The importance of this transition value of Taylor number is that for $Ta < \mathrm{Ta}^{\diamond}$ the bifurcation is forward for the whole domain of overstability. This transition value of Taylor number was evaluated as $Ta^{\diamond} = 21.3$ and its corresponding value of γ is $\gamma^{\diamond} = 3.596$ (see detail as the inset of figure 10). The relaxation time h^{o}_{12} is always positive in the parameter domain considered.

Equation (59) yields at the post-transient state $r^2 = h^{o}_{23}\,\xi_{ov}$ for supercritical values of R, where $h^{o}_{23} = 1/h^{o}_{32}$, providing the solution for r in the form

$$r = \begin{cases} 0 & \forall\, R < R^{(ov)}_{cr} \\ \pm[h^{o}_{23}\,\xi_{ov}]^{1/2} & \forall\, R \geqslant R^{(ov)}_{cr}. \end{cases} \tag{61}$$

Therefore the post-transient amplitude solution is

$$A = r\exp(\mathrm{i}\dot{\theta}t) = \pm(h^{o}_{23}\,\xi_{ov})^{1/2}\exp(\mathrm{i}\dot{\theta}t), \tag{62}$$

where the nonlinear frequency correction, $\dot{\theta}$, is obtained by substituting the corresponding solution of r^2 in equation (60) and is

$$\dot{\theta} = \mathrm{d}\theta/\mathrm{d}t = (m_{21} - m_{31}\,h^{o}_{23})\,\xi_{ov}. \tag{63}$$

It is evident from equations (62) and (47) that a Hopf bifurcation occurs at the critical value of the Rayleigh number associated with overstable convection. The post-transient values of $|A|$ as presented in equation (61) were evaluated in terms of $\log_{10}[|A|/\varepsilon]$ and are presented graphically in figure 11 as a function of γ, for different values of the Taylor number. From the figure, one observes that the solutions diverge as the value of γ approaches the tricritical point. As this happens in the neighbourhood of the CTP a different expansion is needed to investigate the solution there, because the divergence of the amplitude violates the assumptions made regarding the amplitude expansion.

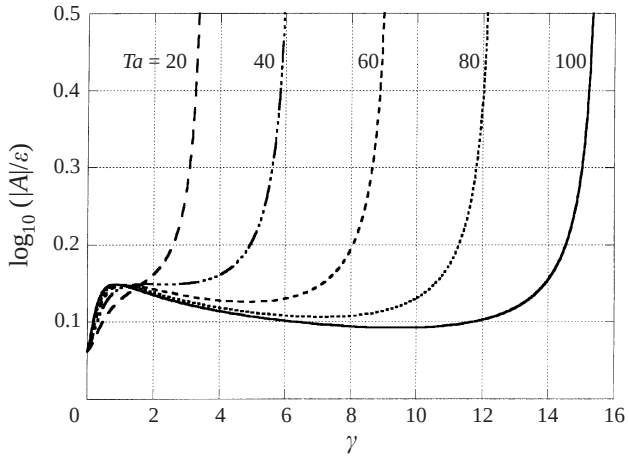

FIGURE 11. Finite-amplitude results for overstable convection: post-transient amplitude as a function of γ for different values of the Taylor number.

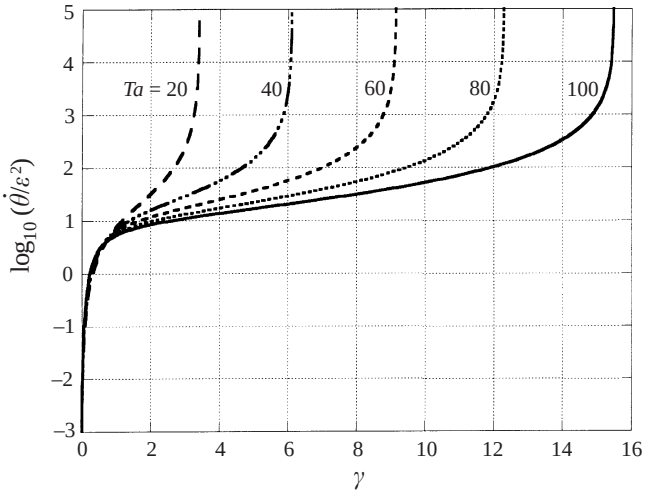

FIGURE 12. Finite-amplitude results for overstable convection: post-transient nonlinear frequency correction as a function of γ for different values of the Taylor number.

The post-transient values of the nonlinear frequency correction were evaluated using equation (63) in terms of $\log_{10}[\dot{\theta}/\xi_{ov}]$ and are presented in figure 12 as a function of γ for different Taylor numbers. It can be observed that the nonlinear frequency correction diverges as $\gamma \to \gamma_{tc}$. It is also observed from figure 12 that, for values of γ which are not small, the frequency correction decreases as the Taylor number increases at the same value of γ.

During the linear stability analysis of overstable solutions the particular case when $\gamma \to 0$ was identified as worth noticing because it produced critical values of Rayleigh numbers and wavenumbers which are independent of Ta (see equation (28) and the text following it). It is of interest to discuss this particular case in the context of the weak nonlinear results as well. Calculating the limit of the coefficients in the amplitude equations (59) and (60) yields the following results: $h^o_{32} \to 3/4$, $m_{21} = m_{31} \to 0$ and $h^o_{12} = (1/\pi^2\gamma) \to \infty$ as $\gamma \to 0$. These results provide a post-transient amplitude and frequency

correction of $|A| \to 2\varepsilon/\sqrt{3}$ and $\dot{\theta} \to 0$ as $\gamma \to 0$. The value of h^o_{12} indicates that the relaxation time diverges as $\gamma \to 0$. Nevertheless, one can conclude that for sufficiently small values of γ ($\gamma \quad 1$) the overstable solution oscillates at the neutral frequency $(Ta/2-1)^{1/2}$ having a post-transient amplitude of $|A| \approx 2\varepsilon/\sqrt{3}$. The time needed to reach the post-transient state is obviously very long, i.e. $O(\gamma^{-1})$. The corresponding heat flux associated with small values of γ is discussed in the next subsection.

4.3. *Heat flux and Nusselt number*

This section is dedicated to estimate the heat flux in terms of the Nusselt number for both stationary and overstable convection by using the evaluated amplitude results. The mean Nusselt number is defined as

$$\overline{Nu} = \frac{1}{l}\int_0^l [wT - \partial T/\partial z]\,\mathrm{d}x, \tag{64}$$

where l is the length of the domain and can be taken as the cell wavelength. However, since

$$\frac{\partial}{\partial z}\int_0^l \left(wT - \frac{\partial T}{\partial z}\right)\mathrm{d}x = 0 \tag{65}$$

it means that the Nusselt number is not a function of z and therefore can be evaluated for convenience at $z = 0$ where $w = 0$.

Substituting the solutions for stationary convection at the different orders after eliminating the slow space scale on the grounds presented in §4.1 yields the following relationship for the stationary convection Nusselt number at steady state:

$$\overline{Nu}^{(st)} = 1 + 2\left[\frac{R}{R^{(st)}_{cr}} - 1\right] + O(\varepsilon^3) \quad \forall\, R \geqslant R^{(st)}_{cr}, \tag{66}$$

where it is obvious that $\overline{Nu}^{(st)} = 1 \,\forall\, R < R^{(st)}_{cr}$, indicating that the convection heat transfer branches off from the conductive heat transfer line (which is parallel to the $R/R^{(st)}_{cr}$ axis) at the critical value of the Rayleigh number. The gradient of the supercritical Nusselt number in the $(\overline{Nu}^{(st)}, R/R^{(st)}_{cr})$-plane has the value of 2. As the critical Rayleigh number for convection in the absence of rotation is smaller than the corresponding Rayleigh number associated with rotation, it can be concluded that as far as stationary convection is concerned the rotation has a retarding effect on heat transfer.

Regarding the heat flux corresponding to overstable convection the Nusselt number is evaluated similarly as for stationary convection with the only difference that here a time average over a cycle is performed as well and therefore the mean Nusselt number has the meaning of average in space as well as in time. To order ε^2 this yields for the post-transient state

$$\overline{Nu}^{(ov)} = 1 + \frac{2\alpha(\alpha+1)\,h^o_{23}}{\pi[(\alpha+1)^2 + \gamma^2\sigma_o^2]}\left[\frac{R}{R^{(ov)}_{cr}} - 1\right] + O(\varepsilon^3) \quad \forall\, R \geqslant R^{(ov)}_{cr}, \tag{67}$$

where $h^o_{23} = 1/h^o_{32}$, $h^o_{32} = h^o_{31}/h^o_{21}$ and h^o_{21}, h^o_{31} are as defined by (56*b*) and (56*d*), respectively. The variation of Nusselt number as a function of γ was evaluated for different values of the Taylor number and is presented in figure 13, in terms of $\log_{10}(\overline{Nu}^{(ov)} - 1)/\xi_{ov}$. We can observe from the figure that for most of the γ-domain the heat flux at a constant value of γ decreases as the Taylor number increases, indicating that the rotation has a retarding effect on heat transfer for overstable convection as well. Nevertheless, this pattern changes for small values of γ, but not necessarily too

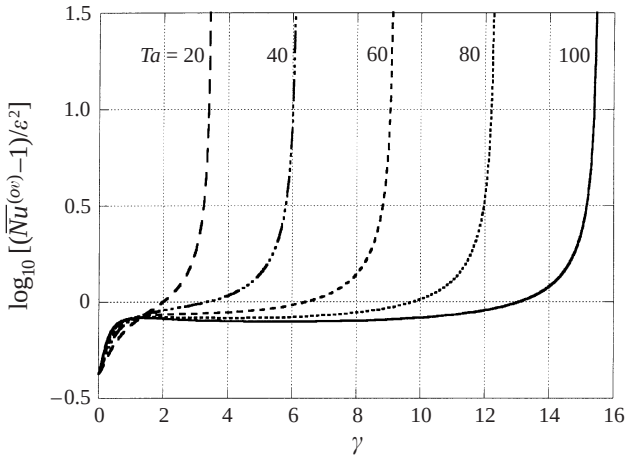

FIGURE 13. Heat transfer results for overstable convection: post-transient Nusselt number as a function of γ for different values of the Taylor number.

small. As the intersection between the curves does not occur at the same value of γ it is difficult to provide an accurate transition point. Nevertheless, it is evident that for small values of γ rotation can enhance the heat transfer.

The particular case of sufficiently small values of $\gamma(\gamma \quad 1)$ was evaluated for the limit $\gamma \to 0$ and provides a mean Nusselt number of $\overline{Nu}^{(ov)} \approx 1+4\varepsilon^2/3\pi+O(\varepsilon^3)$, which is independent of the rotation parameter Ta.

5. Summary and conclusions

The linear stability results indicate that in contrast to the corresponding pure-fluids (non-porous domains) problem, the convection problem in porous media subject to rotation allows overstable solutions without limiting the Prandtl number. In the porous-media problem we find also that the critical wavenumber in the plane containing the streamlines for stationary convection is not independent of rotation, a result which is also distinct from the corresponding case in pure fluids. However, just as in pure-fluids convection, the viscosity in porous-media convection at high rotation rates has a destabilizing effect. The finite-amplitude results show that a pitchfork bifurcation occurs for the stationary convection case and a Hopf bifurcation for the overstable convection, at the corresponding critical values of the Rayleigh number. The finite-amplitude results are used to evaluate the convective heat flux. Although for both stationary and overstable convection the rotation has in general a retarding effect on heat transfer (except for small γ values when overstable convection can enhance the heat transfer), in the stationary convection case this is due only to the fact that instability and convection occurs at a higher Rayleigh number than for the case without rotation. To observe this interesting result we look at the limits of $R_{cr}^{(st)}$ and $\alpha_{cr}^{(st)}$ as the Taylor number approaches infinity or zero. The limit for $Ta \to \infty$ is presented in equation (18), i.e. $R_{cr}^{(st)} \to Ta + O(Ta^{1/2})$ and $\alpha_{cr}^{(st)} \to Ta^{1/2}$ as $Ta \to \infty$, while the corresponding limit for $Ta = 0$ is $R_{cr}^{(st)} = 4$ and $\alpha_{cr}^{(st)} = 1$ as $Ta \to 0$. Substituting these limiting values in the steady-state amplitude solutions yields $\varepsilon C^{(1)} = \sqrt{2}[8(R/R_{cr}^{(st)}-1)]^{1/2}$ for $Ta \to 0$ and $\varepsilon C^{(1)} = 1[8(R/R_{cr}^{(st)}-1)]^{1/2}$ for $Ta \to \infty$. Therefore, for the same relative distance from the corresponding value of $R_{cr}^{(st)}$, there is a 29% reduction in the amplitude from 1.41 to 1 as Taylor number increases from 0 (corresponding to convection in the absence of rotation) to infinity. Nevertheless,

substituting the same limiting values in the expression for the Nusselt number as a function of amplitude, i.e. $\overline{Nu}^{(st)} = 1 + \alpha_{cr}^{(st)}(\varepsilon C_1)^2/4(\alpha_{cr}^{(st)} + 1)$, provides exactly the same result for both $Ta \to \infty$ and $Ta \to 0$, as presented in equation (66). This is so because of the corresponding variation of the critical wavenumber as a function of Ta, a fact which counter-balances the significant reduction of amplitude and its impact on the heat transfer. For overstable convection it was demonstrated that the heat transfer reduction (when the values of γ are not small) is due not only to the stabilizing effect of rotation but also to the fact that for supercritical Rayleigh number values at the same γ value, increasing the rotation rate reduces the heat transfer coefficient. For small values of γ the rotation has an enhancing effect on heat transfer leading to the limiting value of $\overline{Nu}^{(ov)} = 1 + 4\varepsilon^2/3\pi$ for $\gamma \quad 1$, which is the same for all Taylor numbers.

The work described in this paper was partially supported by the Foundation for Research Development through the Competitive Industry Research Grant (CIPM-GUN2034039).

REFERENCES

Bejan, A. 1995 *Convection Heat Transfer*, 2nd Edn. Wiley.

Brand, H. R., Hohenberg, P. C. & Steinberg, V. 1984 Codimension-2 bifurcations for convection in binary fluid mixtures. *Phys. Rev.* A **30**, 2548–2561.

Chakrabarti, A. & Gupta, A. S. 1981 Nonlinear thermohaline convection in rotating porous medium. *Mech. Res. Commun.* **8**, 9–22.

Chandrasekhar, S. 1961 *Hydrodynamic and Hydromagnetic Stability*. Oxford University Press.

Cross, M. C. & Kim, K. 1988 Linear instability and the codimension-2 region in binary fluid convection between rigid impermeable boundaries. *Phys. Rev.* A **37**, 3909–3920.

Friedrich, R. 1983 Einfluß der Prandtl-Zahl auf die Zellularkonvektion in einem rotierenden mit Fluid gesättigten porösen Medium. *Z. Angew. Math. Mech.* **63**, T246–T249.

Jou, J. J. & Liaw, J. S. 1987*a* Transient thermal convection in a rotating porous medium confined between two rigid boundaries. *Intl Commun. Heat Mass Transfer* **14**, 147–153.

Jou, J. J. & Liaw, J. S. 1987*b* Thermal convection in a porous medium subject to transient heating and rotation. *Intl J. Heat Mass Transfer* **30**, 208–211.

Newell, A. C. & Whitehead, J. C. 1969 Finite bandwidth, finite amplitude convection. *J. Fluid Mech.* **38**, 279–303.

Nield, D. A. & Bejan, A. 1992 *Convection in Porous Media*. Springer.

Palm, E. & Tyvand, A. 1984 Thermal convection in a rotating porous layer. *Z. Angew. Math. Phys.* **35**, 122–123.

Patil, P. R. & Vaidyanathan, G. 1983 On setting up of convection currents in a rotating porous medium under the influence of variable viscosity. *Intl J. Engng Sci.* **21**, 123–130.

Rudraiah, N., Shivakumara, I. S. & Friedrich, R. 1986 The effect of rotation on linear and non-linear double-diffusive convection in sparsely packed porous medium. *Intl J. Heat Mass Transfer* **29**, 1301–1317.

Schöpf, W. & Zimmermann, W. 1993 Convection in binary fluids: Amplitude equations, codimension-2 bifurcation, and thermal fluctuations. *Phys. Rev.* E **47**, 1739–1764.

Segel, L. A. 1969 Distant side-walls cause slow amplitude modulation of cellular convection. *J. Fluid Mech.* **38**, 203–224.

Steinberg, V. & Brand, H. R. 1984 Amplitude equations for the onset of convection in a reactive mixture in a porous medium. *J. Chem. Phys.* **80**, 431–435.

Vadasz, P. 1993 Three-dimensional free convection in a long rotating porous box. *J. Heat Transfer* **115**, 639–644.

Vadasz, P. 1994 Stability of free convection in a narrow porous layer subject to rotation. *Intl Commun. Heat Mass Transfer* **21**, 881–890.

VADASZ, P. 1995 Coriolis effect on free convection in a long rotating porous box subject to uniform heat generation. *Intl J. Heat Mass Transfer* **38**, 2011–2018.

VADASZ, P. 1996*a* Stability of free convection in a rotating porous layer distant from the axis of rotation. *Transfer in Porous Media* **23**, 153–173.

VADASZ, P. 1996*b* Convection and stability in a rotating porous layer with alternating direction of the centrifugal body force. *Intl J. Heat Mass Transfer* **39**, 1639–1647.

VERONIS, G. 1958 Cellular convection with finite amplitude in a rotating fluid. *J. Fluid Mech.* **5**, 401–435.